Computational fluid dynamic analysis on forced convective heat transfer using nanofluid TiO_2 by using Ansys

Dinesh Kumar Verma
Dept. of Mechnical engineering
NITM
Gwalior, India

Prof.P.S. Dhakad
Dept. of Mechnical engineering
NITM,
Gwalior, India.

Abstract*—Transfer of heat energy is used in a wide range of industrial processes. Heat must be inserted, eliminated, or transferred from one cycle source to another throughout any industrial facility and has become a main task to industrial requirement. Such systems give a means of heating/cooling for energy recovery and plant gas. The thermo-physical properties of nanofluids are important for predicting heat transfer behaviour. Management of manufacturing and energy-saving viewpoints is extremely important. Nanofluids are of significant commercial importance. Effect of fixed volume wall temperature concentration on Nusselt number (NN) is illustrated in figures below, in range of 60 to 90 ° C. There is a significant scope for improvement in thermal transfer properties in comparison with normal suspension, millimeter & micron particle fluids. For this scenario, most experts believe that the optimal cooling system efficiency may be obtained at a nanoparticles low volume fraction (b1 percent). At around the same time, there are still some issues and difficulties with respect to heat transfer improvement processes & real implementations on engine vehicles. Modern nanofluid technology for the engine cooling system is still in its first phase & requires more progress.

Keywords: Heat Transfer,Nano Fluids,Tio₂

I. INTRODUCTION

The transfer of heat energy is part of a broad range of industrial processes. Heat should be added, removed or transferred from one source of processes to another throughout any industrial facility and this is now an important task for the industry. Both processes give a good means of heating and cooling of the fluid. In an industrial process, improvement of heating/cooling can create energy savings, reduce process times, increase heat ratio and extend the life of equipment. Those procedures are even qualitatively influenced by the operation of increased heat transfer (HT). The development of high-performance thermal systems to HT systems has now become popular. A work variety was done to understand the efficiency of HT to their practical application to improve HT. This generated an important demand for novel technologies to improve HT through the production of heat flow processes. [1, 3]

HT performance of liquids is restricted with their low thermo-physical characteristics in comparison to solids. Nanofluid is the primary cause of adding solid particles with a lower level of fluid. Recently, dispersion into a base fluid, like ethylene glycol, water or glycerol of solid metallic and non-metallic materials, has become an interesting topic. Basic fluids in automotive radiators have for many years been utilized as traditional coolants but these fluids have poor thermal conductivity. This has led scientists to look for liquids with higher thermal conductance than traditional refrigerants because of their low thermal conductivity. Instead of the widely used basal fluids, nanofluids were used. The range of flow rates for all experiments ranged from 2 to 6 LPM by fluid inlet temperature increasing. Results illustrated that nanofluids increased HT relative to pure water by 40 percent. A statistical study was performed in a flat tube in a car radiator by laminar HT with CuO & Al2O3 ethylene glycol and water [4].

Starting with their initial vision, nanofluids have been closer to an engineering reality more than a decade ago. Because of recognition in practical applications of nanofluids, the last decade has given more attention to improved convective HT performance of nanofluids. In several engineering applications, heat exchangers are commonly used for applications such as energy, chemical & food industry processing, environmental engineering, waste thermal recovery & air conditioning & refrigeration. Researchers have also been very conscious of the characteristics of flow/heat transport in microchannels and microtube, as microelectro mechanical systems (MEMS) and micro-total analyzes have evolved rapidly. This has significant impacts on techniques of microelectronic cooling, micro heat exchanger, bioengineering, the human genome project, medical engineering and so on. This review article is intended to sum up the potential for thermal transfer of nanofluids in experimental and numerical work as well as in effect of nanoparticles ' concentration and diameter and form of cross-sectional tubes [5].

Enhanced channel thermal efficiency can be enhanced with heat transfer techniques. Heat transfer methods may be categorized into 3 broad methods: passive techniques that don't require external power like swirl flow devices, rough surfaces, extended surfaces, treated surfaces, surface tension devices, displaced enhancement devices, additives & coiled tubes like nanoparticles; active methods that require exterior power to allow desired flow modification to enhance HT like mechanical aids, suction, electrostatic fields, surface vibration, jet impingement, fluid vibration, & injection; compound methods that are a mix of two or more of above-mentioned method. It was achieved by shear rate & mass fraction of nanoparticles. Mateecsu, Luciu, introduced an experimentally & numerically dual-tube coaxial heat exchanger heated through solar energy with Al_2O_3 (aluminum oxide) nanofluid. Their results show that nanofluid transmission performance is higher than the base fluid. TiO2 (Titanium dioxide) & SWCNH (single-wall carbon nanohorn) have already & used as a basic fluid for two other non-like substances. Results showed viscosity equations of the empirical correlation. The turbulent flow of nanofluids CuO, Al 2O3 & TiO2 flowing by a 2D conduit in a constant heat flow condition with different volume concentrations was numerically analyzed [6].

Nanotechnology has attracted the interests of researchers to be one of the important research fields that lead to the next major industrial revolution in the future. A massive research effort has been done to investigate the thermal transport properties of colloidal suspensions of nano-sized solid particles known as nanofluids. Traditional working fluids

have inherently low thermal conductivity relative to solid particles. Recent works found that the nanoparticle's existence in the fluids increases the thermal conductivity of fluid which results in enhancing heat transfer properties. With their special features, nanofluids emerge like a new generation of working fluids in heat exchanging applications. Extensive studies have been accomplished experimentally and numerically to consider influential factors of thermal conductivity & HT coefficient of nanofluids. Several factors have been verified, namely types of nanoparticles and base fluids, nanoparticle volume concentration, nanoparticle size and etcetera. Previous researches have shown that the introduction of nanoparticles into base fluid significantly increases convective HT performance in evaluation by pure base fluids. Based on an earlier investigation on nanofluid regarding thermo-physical properties & heat transfer coefficient on a single type of nanoparticles, graphene-based nanofluids provided a remarkable heat transfer coefficient. [7].

II. LITERATURE SURVEY

Palaniappan et al. (2019) Presented automobile radiators ' thermodynamic efficiency with ethylene glycol (40%), water (60%)–fly ash nanofluid. This explores the effect of nanofluid flow rate and fly ash concentration on HT parameters (e.g. total coefficient of heat transfer & heat transfer), energy transfer parameters (e.g. performance index and pumping power) & energy performance parameters (e.g. energy devastation rate and energy efficiency) [8].

Xian et al. (2019) Recent analysis on the effect of nanofluid deployment, in particular in vehicle cooling as well as further HT applications like electronic cooling system, solar collector, flow boiling & thermal energy storage system has been attempted. In the field of simulation, testing devices and even real car engine experiments, thermophysical properties and HT performance of nanofluids will be thoroughly discussed. Models and associations for measuring thermophysical properties used by past researchers are also included. [9].

Saxena et al. (2018) concentrate on experimental & numerical tests containing different nano-coolants such as CuO, Al2O3, TiO2 & SiO2 that previous scientists conducted on metallic or non-metallic oxide nano-coolants. The analysis concentrates on acceptable volumetric concentrations, nano-particle sizes used by researchers & analytical applications. This analysis will be useful for researchers working in the field of nanotechnology applications in developing heat transfer fluids. For preparation and stability, characterization and applications for overcoming challenges many researcher works are nevertheless still important. [10].

Micali et al. (2018) Four strokes single-cylinder engine experimental program aims to determine the utilization of nanofluids as a viable alternative for rising engine peak engine temperature instead of water. The thermal conductivity of nanofluids of this kind in evaluation to traditional fluids was higher due to added CuO nanoparticles at several concentrations within basis fluids. [11].

Boopathi et al. (2018) firstly preparation of novel composite fly ash nanofluid was made for 0.2-2.0% volume concentration of fly ash particles and mass density, thermal conductivity, specific heat, dynamic viscosity of fly ash nanofluid were measured using standard methods and compared with thermo-physical properties of Alumina (Al_2O_3), Copper Oxide (CuO), Ferrous Oxide (Fe_2O_3), Silicon Oxide (SiO_2), Titanium Oxide (TiO_2) nanofluids for similar % volume concentration. The average grain size of nanoparticles taken for the study was 50nm. 2 step techniques were utilized to prepare fly ash nanofluid. A mixture of 60 percent deionized water 40 percent ethylene glycol was used as a base fluid and sodium dodecyl benzyl sulfate as a surfactant for stabilizing the nanoparticles. [12].

According to **Asli et al. (2018)** To structure a decision issue & attribute weights to criteria, the analytic hierarchy process is utilized. Three different nanofluid types were assessed (Cu-water, NiO-water and CuO-water). Very important thermophysical properties of nanofluid are measured as thermal conductivity, & also as thermophysical properties in assessed nanofluid, Cu-water is determined to be the most suitable coolant. [13].

As per **Shete et al. (2018)** To order to reduce its impact on the environment and reduce global consumption of fuel, the efficiency of an automotive system should be improved. A new foundation for technology integration and innovation is the implementation of nanofluid technology using nano lubricants within various automotive subsystems. For nanofluids, nanoparticles lead to a greater mixing flow & thermal conductivity for contrast with pure fluid. [14].

Wong et al. (2017) focused on the presentation of a broad range of applications involving nanofluids, recognizing their controllable, improved heat transfer properties and the special characteristics which nanofluids have to make them suitable for those applications. [15].

Sidik et al. (2017) The analysis starts with a description of preparation procedures & enhanced thermal conductivity of nanoparticular fluids. Nanofluids can demonstrate the thermal performance of a vehicle engine. It also emphasized the key use of radiator nanofluids and the use of lubricants to improve the efficiency of heat removal from the vehicle engine.[16]

III. PROPOSED METHODOLOGY

An inclusive application of nanofluids for vehicular cooling engines was described in this report. Nanofluids have shown a broad range of available references in the development of modern engines. Nanoparticles may be dispersed in fluid for a cooling system of radiators to increase the liquid's thermal conductivity. In comparison, it increases heat efficiency & decreases friction by the presence of nanoparticle materials in the radiator. Nevertheless, it remains unknown about the optimal amount of nanoparticles. The application of nanoparticles in a traditional radiator is an alternative means of cooling an automotive engine system. The coefficient of heat transfer in relation to the original coolant may be increased by up to 50%; however, the pressure drop issue limits the cooling systems performance. In this case, many researchers believe that an optimum cooling system efficiency may be obtained by a small fraction (b1 percent) of nanoparticles. At the same time, the developments in heat transfer mechanisms and practical applications on motor vehicles remain troublesome and difficult. Recent nanofluid work for engine cooling systems remains at its primary phase and needs further development. A no. of TiO2 nanoparticles distributed in water was therefore defined to be a friction factor & forced HT in a car radiator. in this study 4, several nanofluids (1%, 2%, 3% & 4%) were used to check for resulting thermal properties, with differences in volume.

A. PHYSICAL MODEL

The automobile radiator utilized in this experiment, which includes a hydraulic diameter (Dh=4.5 mm) & a flat tube (L=500 mm) is shown in Figure 1. Number of Reynolds measured on a hydraulic diameter (Dh):

$$D_h = \frac{4 \times Area}{Perimeter}$$

$$D_h = \frac{4 \times [\frac{\pi}{4}d^2 + (D-d) \times d]}{\pi \times d + 2 \times (D-d)}$$

Reynolds number (Re) is defined as:

$$Re_D = \frac{\rho \times D_h \times u}{\mu}$$

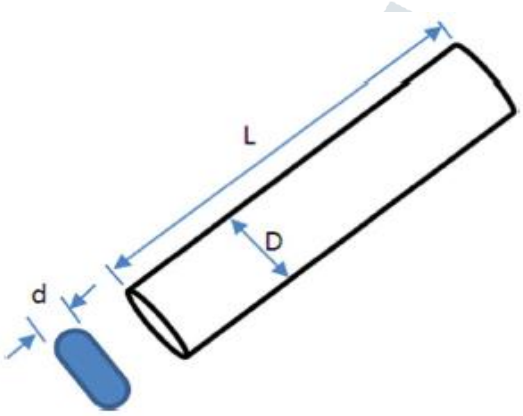

Figure 1: Flat tube of radiator

B. ASSUMPTIONS ASSUMED IN STUDY

Various assumptions have been made on automotive cooling system operational conditions [16 & 17]:

1. Standard, Newtonian turbulent fluid & incompressible flows by constant thermo-physical nanofluid properties assumed.
2. In axial direction & wall thickness of tubes, heat conduction was also overlooked.

C. GOVERNING EQUATIONS

A single-phase approach may be used with infinitesimal (under 100 nm) solid particles, which is why the single-phase method has been adopted for modeling of nanofluids. By following equations thermal properties of nanofluid may be determined:

$$\rho_{nf} = \left(\frac{\phi}{100}\right)\rho_p + \left(1 - \frac{\phi}{100}\right)\rho_f$$

$$C_{nf} = \frac{\frac{\phi}{100}(\rho C)_p + (1 - \frac{\phi}{100})(\rho C)_f}{\rho_{nf}}$$

$$k_{nf} = (1 + 3\Phi)k_f$$

$$\mu_{nf} = (1 + 2.5\Phi)\mu_f$$

Where ρ, C, μ and k are density, thermal conductivity, viscosity & specific heat capacity, correspondingly, as well as subscripts, nf, p,& f, show nanofluid, fluid, and solid properties, correspondingly. [18]

$$\nabla \cdot V = 0$$

$$V_x\frac{\partial V_z}{\partial x} + V_y\frac{\partial V_z}{\partial y} + V_z\frac{\partial V_z}{\partial z} = -\frac{1}{\rho}\frac{\partial P}{\partial z} + \upsilon\frac{\partial^2 V_z}{\partial z^2} + g_z$$

$$V_x\frac{\partial T}{\partial x} + V_y\frac{\partial T}{\partial y} + V_z\frac{\partial T}{\partial z} = \alpha\frac{\partial^2 T}{\partial z^2}$$

D. FEM MODELLING

Creation of geometry:

Geometry was produced in the Ansys workbench Design modeler.

Working fluid is flowing in the automobile radiator. For creating the fluid zone the extrude option in the design modeler is used. For using an extrude option and a sketch is required. The profile is created in the XY plane. The profile here is a flat tube. The path here is a straight line along the Z-axis. Profile is created in the XY plane. The flat tube is generated by giving a profile using the extrude option. In the details, the type is changed to fluid from solid.

E. DATA PROCESSING

FLUENT estimates Nusselt no. as ensues

Outlet air temperature T_{out} was computed as a mass average temperature at the outlet position of the calculation domain.

$$T_{out} = \frac{\int T\rho\vec{u}.d\vec{A}}{\int \rho\vec{u}.d\vec{A}} = \frac{\sum_{i=1}^{n} T_i \rho_i \vec{u}_i . \vec{A}_i}{\sum_{i=1}^{n} \rho_i \vec{u}_i \vec{A}_i}$$

Defined and measured in function of Reynolds number & geometric parameters was dimensionless no. of air-side HT in finned tube bank. In many cases, NN & Stanton numbers are utilized to represent HT coefficient & characteristic length is not the same.

In here the Nu number was used as:

$$Nu = \frac{hd}{k_a}$$

Static pressure at inlet and outlet of computational domain we re-evaluated as

$$p_{in,out} = \frac{\int p d\vec{A}}{\int d\vec{A}} = \frac{\sum_{i=1}^{n} p_i \vec{A}_i}{\sum_{i=1}^{n} \vec{A}_i}$$

F. CFD STEPS

To simulate, the following analysis processes are completed.

1. Initiate FLUENT by 3D solver
2. Read an obtainable grid file & feed into FLUENT
3. Check grid (for example, cell volume, no. of nodes, concerning dimension of calculation domain & area of every cell)
4. Select the appropriate type of solver:

For the solution of the discrete equation, Fluent provides 3 types of solvers. In general, special features of analysis are discussed by "segregated solvers" (incompressible & moderately compressible flows). One solver resolves sequentially (e.g. separated by one another) continuity, dynamics, energy & species equations, and other 2 solvers concurrently (that is coupled together) solve these equations for a high-speed compressible flow.

5. Select model: Choose k-ε (RNG) model to measure the flow area. Set standard wall functions for near fin treatment. Activate the energy equation to connect heat transfer (convection & conduction).
6. Describe properties of the following material
7. Define boundary conditions
8. Define the control parameter
9. Initialization of flow field.
10. Compute solution.
11. Result Saved

IV. EXPERIMENTAL RESULTS

Effect of nanofluid concentration:

NUSSELT NUMBER

Figure 2 illustrated temperature profiles at several Reynolds number. Furthermore, the minimum temperature is 300 K and 333 K at Reynolds number is 10000for TiO_2.

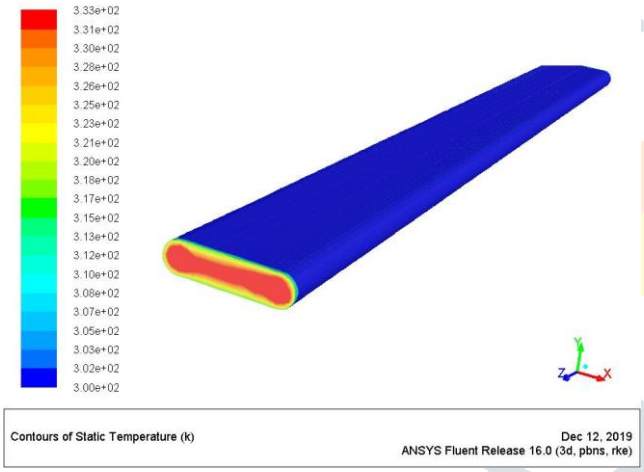

Fig.2: Contour of temperature at Reynolds number (Re = 10000) for TiO_2

Figure 3 illustrated temperature profiles at different Reynolds numbers. Furthermore, the minimum temperature is 300 K and 343 K at Reynolds number is 10000 for Ag/HEG.

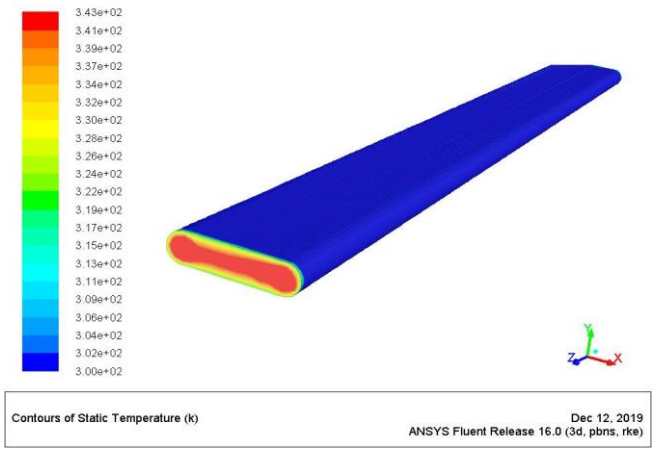

Fig.3. Contour of temperature at Reynolds number (Re = 10000) for Ag/HEG

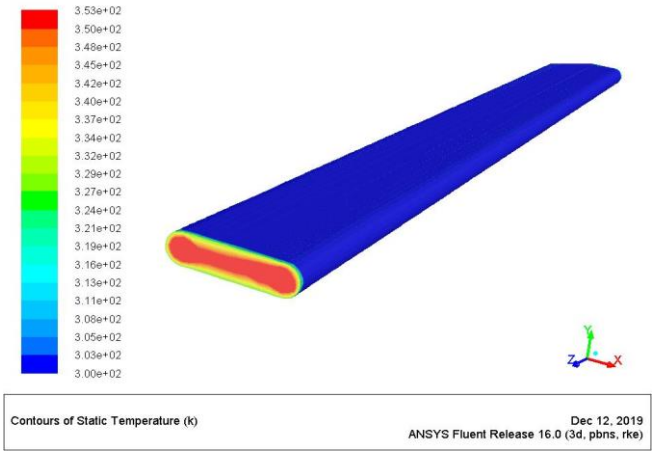

Fig. 4: Contour of temperature at Reynolds number (Re = 10000) for SiO_2

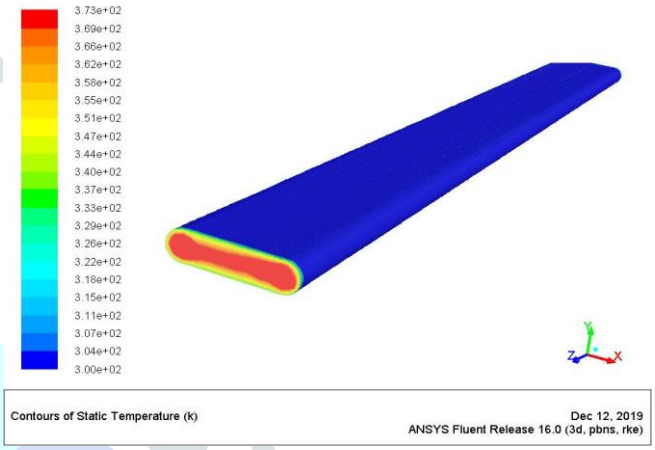

Fig. 5: Contour of temperature at Reynolds number (Re = 10000) for Al_2O_3

Figure 4 illustrated temperature profiles at different Reynolds numbers. Furthermore, the minimum temperature is 300 K and a maximum temperature of 353 K at Reynolds number is 10000 for SiO_2.

Figure 5 illustrated temperature profiles at different Reynolds numbers. Furthermore, the minimum temperature is 300 K and a maximum temperature of 373 K at Reynolds number is 10000 for Al_2O_3.

Table 1: Nusselt number at different nano concentration for TiO_2

Reynolds number	TiO_2				
	Pure water	1%	2%	3%	4%
	Nusselt number				
10000	28.42	40.12	48.63	53.24	61.29
20000	34.63	52.26	57.42	61.14	69.32
40000	45.29	56.42	62.36	68.74	73.47
60000	55.01	64.35	71.58	77.26	82.69
80000	62.58	75.29	78.82	83.45	89.17

100000	69.74	86.44	92.15	97.53	105.36

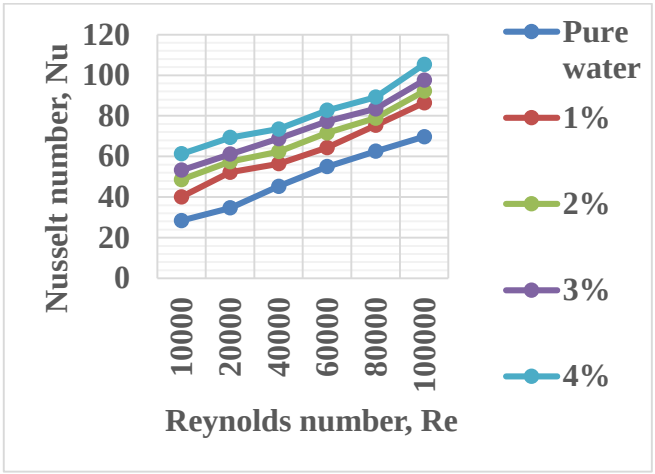

Fig.6: Nusselt number at different nano concentration for TiO_2

In Figures, 6 effects on the amount of Nusselt of different volume concentrations is shown in range 1 to 4 percent of volume nanoparticles. The results show that nanofluid is the highest Nusselt in all Reynolds numbers with 4 percent of highest volume concentration. An increase in the concentration of nanofluid volume explanation for Nusselt is the rise in the thermal conductivity of the fluid.

Table 2: Nusselt number at different nano concentration for Ag/HEG

Reynolds number	Ag/HEG				
	Pure water	1%	2%	3%	4%
	Nusselt number				
10000	28.42	59.08	65.48	78.69	88.06
20000	34.63	68.72	77.17	84.28	93.11
40000	45.29	75.02	81.25	89.19	102.28
60000	55.01	82.19	86.36	96.52	115.62
80000	62.58	88.67	92.08	105.39	128.57
100000	69.74	93.56	97.63	119.58	135.74

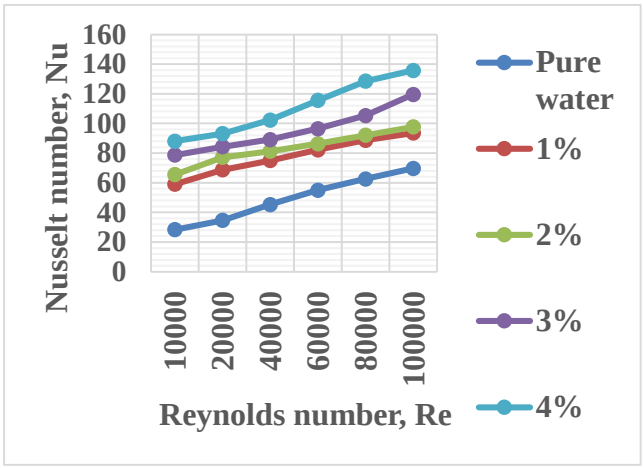

Fig. 7: Nusselt number at different nano concentration for Ag/HEG

Figure 7 of nanoparticle volume concentration range shows the effect of various volume concentrations on NN from 1 to 4%. Studies have shown that nanofluid is the highest NN in all Reynolds numbers with 4 percent of highest volume concentration in Nusselt The explanation for NN with an increase in nanofluid volume concentrations increases the thermal conductivity of the fluid.

Table 3: Nusselt number at different nano concentration for SiO_2

Reynolds number	SiO_2				
	Pure water	1%	2%	3%	4%
	Nusselt number				
10000	28.42	43.25	52.17	63.48	77.29
20000	34.63	61.04	68.04	77.34	85.47
40000	45.29	69.11	75.23	83.49	95.63
60000	55.01	77.34	83.48	92.08	111.37
80000	62.58	82.66	91.37	98.72	119.73
100000	69.74	89.51	95.82	110.42	128.48

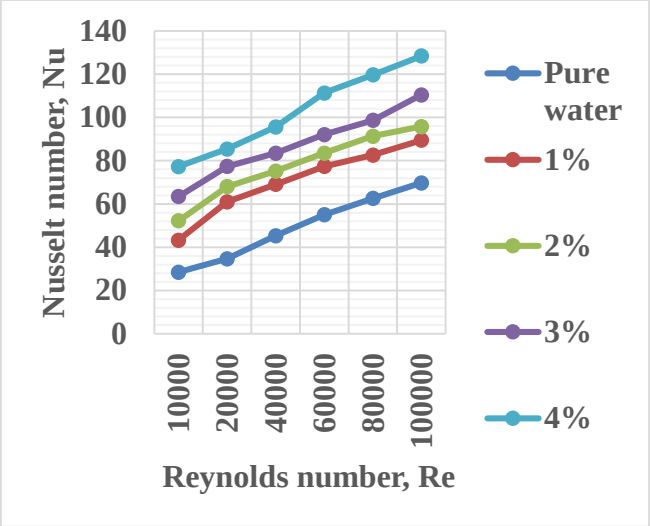

Fig. 8: Nusselt number at different nano concentration for SiO_2

The effect on NN of different concentrations of volume is shown in Fig. 8 at a volume concentration of 1 to 4 percent in nanoparticles. Results indicated that nanofluid is the highest NN in all Reynolds numbers with a 4% maximum volume. The reason for NN's rise in nanofluid volume concentration increases the thermal conductivity of liquid.

Table 4: Nusselt number at different nano concentration for Al_2O_3

Reynolds number		Al_2O_3			
	Pure water	1%	2%	3%	4%
		Nusselt number			
10000	28.42	52.13	60.42	68.39	77.24
20000	34.63	63.74	71.29	79.35	86.07
40000	45.29	69.42	78.36	83.81	96.34
60000	55.01	79.87	82.59	92.68	108.57
80000	62.58	83.58	89.41	100.56	119.63
100000	69.74	92.26	94.84	109.27	127.52

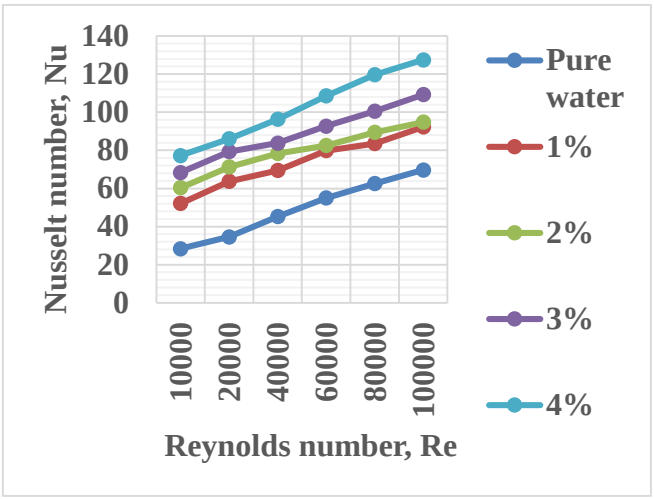

Fig. 9: Nusselt number at different nano concentration for Al_2O_3

Several volume concentrations effect on NN is illustrated in fig. 9 at a range of 1 to 4 % nanoparticle volume concentration. Results illustrated that nanofluid has the highest NN with 4% highest volume concentration at all Reynolds numbers. The reason for the rising of NN by enhancing of volume concentration of nanofluid is increasing fluid thermal conductivity.

A. FRICTION FACTOR (FF)

Contour of pressure drop at specific no. of Reynolds as well as volume of nanofluids is illustrated in figure 4.5-4.8. The pressure drop with NN will necessarily be investigated to apply hybrid nanofluids in industrial applications. Figure 10-13 shows CFD data of a pressure drop on the Reynolds number. The pressure drop decreases by 13 percent as the number of Reynolds rises by 13 percent because of velocity in tube increases. Likewise, hybrid nanofluid fractions volume fractions are subject to little pressure decrease penalties due to increased nanofluid viscosity by 14 percent. Numerical data on sample pressure reduction are consistent with literature [19].

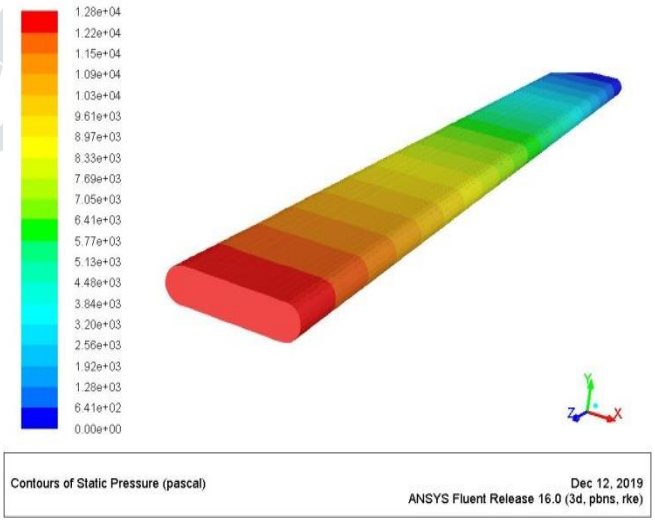

Fig. 10: Contour of pressure at Reynolds number (Re = 10000) for TiO_2

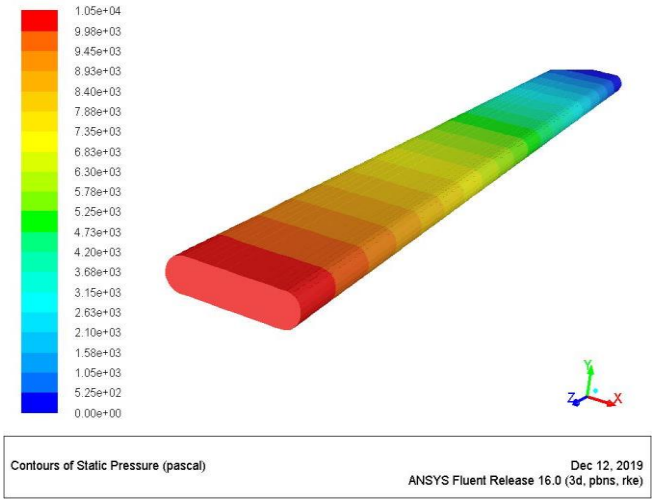

Fig. 11: Contour of pressure at Reynolds number (Re = 10000) for Ag/HEG

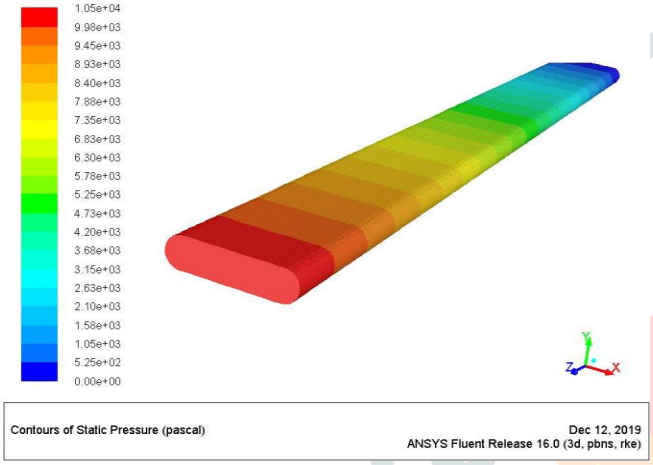

Fig. 12: Contour of pressure at Reynolds number (Re = 10000) for SiO_2

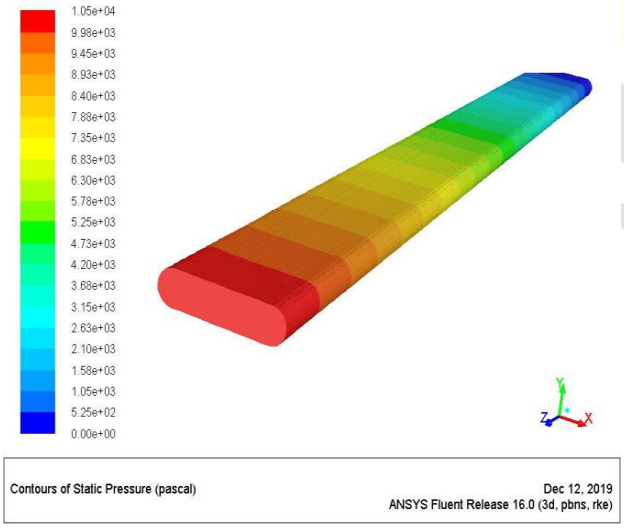

Fig. 13: Contour of pressure at Reynolds number (Re = 10000) for Al_2O_3

Table 5: Friction factor at different nano concentration for TiO_2

Reynolds number	TiO_2				
	Pure water	1%	2%	3%	4%
	Friction factor				
10000	0.215	0.323	0.337	0.354	0.383
20000	0.156	0.257	0.286	0.311	0.332
40000	0.132	0.204	0.249	0.277	0.301
60000	0.123	0.169	0.213	0.253	0.286
80000	0.117	0.143	0.189	0.234	0.263
100000	0.109	0.122	0.166	0.211	0.244

Table 6: Friction factor at different nano concentration for Ag/HEG

Reynolds number	Ag/HEG				
	Pure water	1%	2%	3%	4%
	Friction factor				
10000	0.231	0.331	0.342	0.365	0.395
20000	0.167	0.268	0.297	0.321	0.348
40000	0.144	0.216	0.258	0.285	0.315
60000	0.135	0.182	0.225	0.262	0.292
80000	0.124	0.155	0.196	0.243	0.275
100000	0.115	0.138	0.178	0.22	0.258

Table 7: Friction factor at different nano concentration for SiO_2

Reynolds number	SiO_2				
	Pure water	1%	2%	3%	4%
	Friction factor				
10000	0.228	0.328	0.339	0.362	0.39
20000	0.168	0.263	0.291	0.319	0.342
40000	0.142	0.211	0.250	0.281	0.308
60000	0.124	0.175	0.219	0.259	0.290
80000	0.110	0.151	0.191	0.238	0.272
100000	0.105	0.132	0.172	0.218	0.248

Table 8: Friction factor at different nano concentration for Al_2O_3

Reynolds number	Al_2O_3				
	Pure water	1%	2%	3%	4%
	Friction factor				
10000	0.225	0.228	0.335	0.354	0.372
20000	0.152	0.213	0.284	0.321	0.336
40000	0.142	0.204	0.246	0.275	0.321
60000	0.120	0.162	0.202	0.242	0.286
80000	0.108	0.148	0.184	0.231	0.279
100000	0.101	0.129	0.167	0.211	0.232

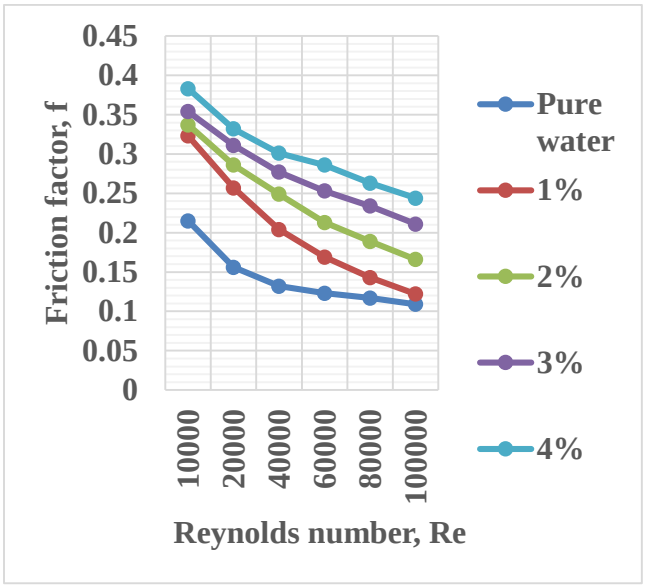

Fig. 14: Variation of friction factor at different nano concentration for TiO_2

The findings show that at 4% highest volume concentration, nanofluid (TiO2) has the highest FF at all Reynolds numbers. The explanation for improving FF by increasing nanofluid volume concentration increases viscosity of fluid which decreases fluid movement. With -Reynolds number, FF of all volume concentrations reduces but with pure water lowest FF is received.

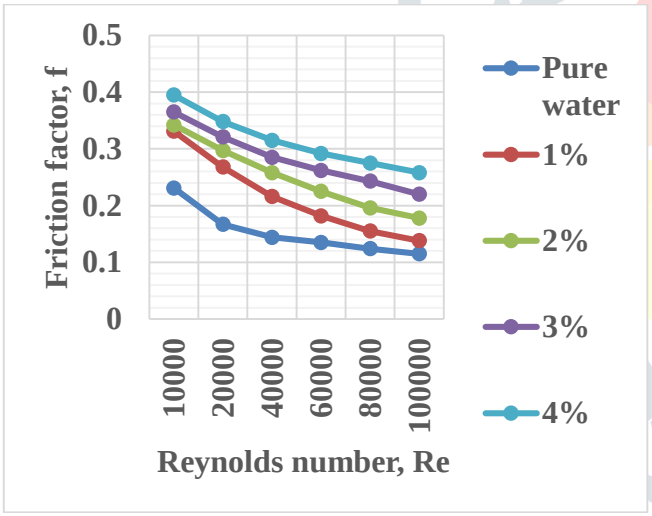

Fig. 15: Variation of friction factor at different nano concentration for Ag/HEG

The results showed that at every Reynold number nanofluid (Ag / HEG), at the highest volume concentration of 4 percent, has the highest FF. This improves fluid viscosity by increasing the volume of nanofluid concentration as well as reduces the movement of fluid. With the increasing number of Reynolds FF for all volume, concentrations reduce and the lowest FF is associated with pure water.

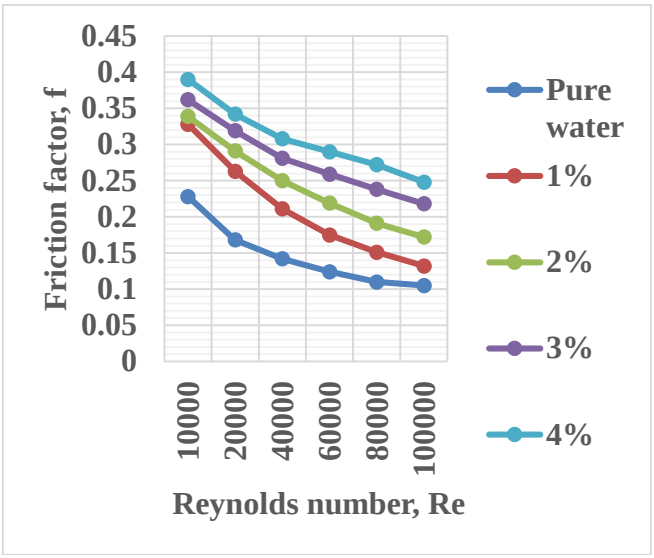

Fig. 16: Variation of friction factor at different nano concentration for SiO_2

The findings have shown that nanofluid (SiO2) has the highest FF of 4% at all Reynolds numbers at its highest concentration. The explanation of why FF increases with the volume of nanofluid concentration increases fluid viscosity that decreases fluid movement. With an improved Reynold numbers FFs for every volume decrease and the lowest FF for pure water is obtained.

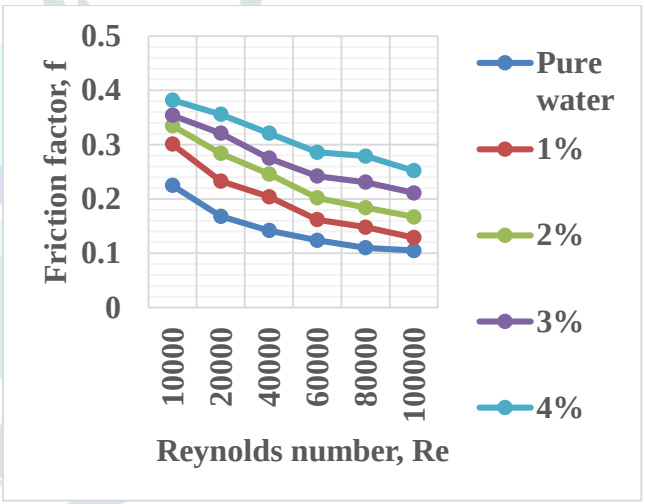

Fig. 17: Variation of friction factor at different nano concentration for Al_2O_3

Results have shown the highest volume of 4 percent nanofluid (Al2O3) to have the highest FF at any Reynolds number. The explanation of why FF is increased by increasing nanofluid volume concentration increases the viscosity of the fluid, minimizing the fluid movement. For the increasing number of Reynolds and the lowest FF for pure water, FF for all volume concentrations decreases.

B. Effect of the wall temperature

The effect of wall temperature of fixed volume concentration on NN is illustrated in the below figures at a range of 60– 90°C.

C.NUSSELT NUMBER

Table 4.4 shows the simulation result of the impact of inlet temp. on NN of TiO_2 nanofluid by 1% volume concentrations

Table 9: Nusselt number at different wall temperature for TiO_2

Reynolds number	TiO_2				
	Pure water	60°C	70°C	80°C	90°C
	Nusselt number				
10000	28.42	40.12	42.51	49.65	58.58
20000	34.63	52.26	55.68	58.34	63.69
40000	45.29	56.42	59.47	62.11	70.37
60000	55.01	64.35	68.29	75.37	79.53
80000	62.58	75.29	78.56	81.24	87.24
100000	69.74	86.44	90.42	95.65	98.57

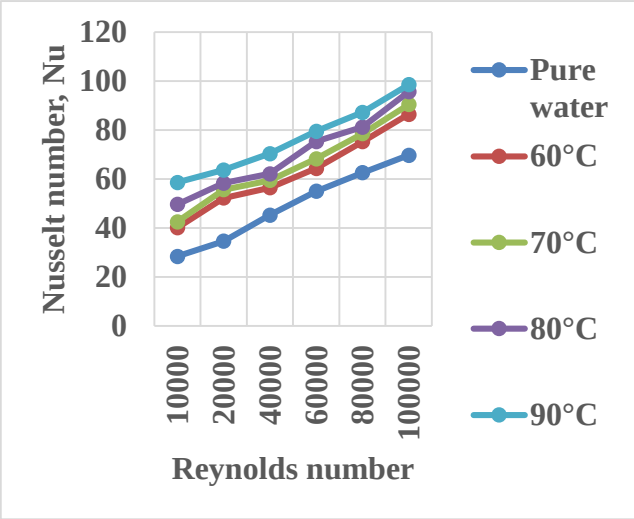

Fig. 18: Variation of Nusselt number at different wall temperature for TiO_2

It emerged that there is an important impact of nanofluid volume concentrations on NN and the effect of inlet temp. on NN.

Table 10: Nusselt number at different wall temperature for Ag/HEG

Reynolds number	Ag/HEG				
	Pure water	60°C	70°C	80°C	90°C
	Nusselt number				
10000	28.42	52.28	60.18	74.22	82.16
20000	34.63	60.32	74.37	80.28	89.71
40000	45.29	72.64	79.24	83.39	92.39
60000	55.01	79.82	82.33	94.24	105.82
80000	62.58	85.57	90.48	98.19	118.66
100000	69.74	92.36	95.66	109.28	128.42

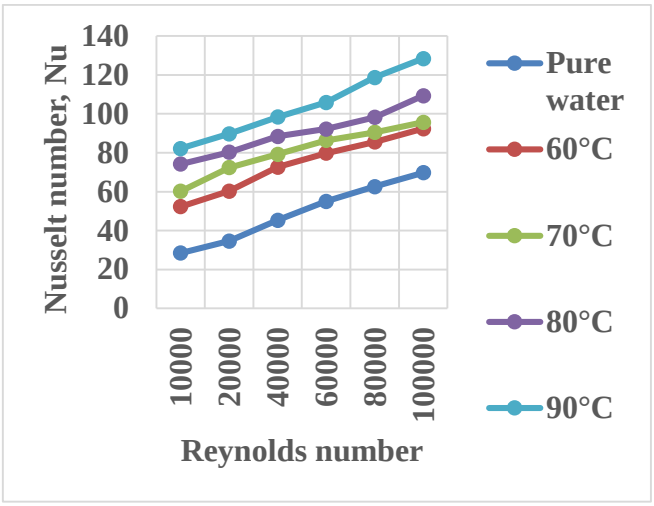

Fig. 19: Variation of Nusselt number at different wall temperature for Ag/HEG

The impact on NNs of various wall temperatures is shown in the figure. 19. Similar behavior, by an increase in volume & Reynolds numbers, is observed to NN. Nusselt number increases by increasing of several wall temperature & Reynolds number. It may be seen that the average Nusselt value for wall temperatures is 90 ° C compared to other types & pure water.

Table 11: Nusselt number at different wall temperature for SiO_2

Reynolds number	SiO_2				
	Pure water	60°C	70°C	80°C	90°C
	Nusselt number				
10000	28.42	40.35	49.67	58.24	72.59
20000	34.63	58.74	64.29	72.57	81.26
40000	45.29	66.52	70.33	79.19	90.13
60000	55.01	73.14	81.28	83.48	92.27
80000	62.58	79.26	88.47	92.62	104.53
100000	69.74	83.67	90.12	107.82	117.18

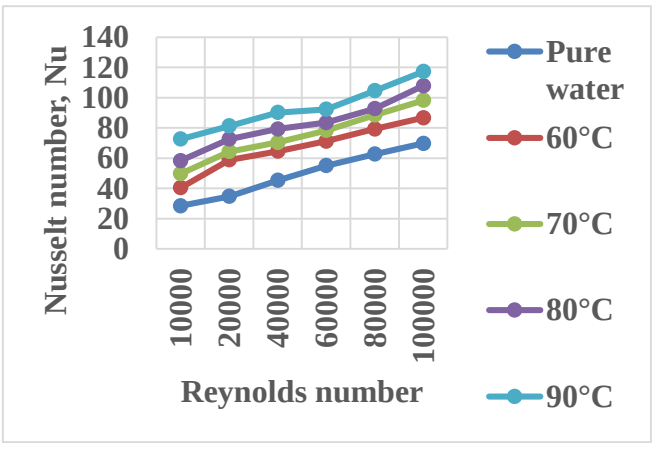

Fig. 20: Variation of Nusselt number at different wall temperature for SiO_2

The effect of different wall temperatures on NN is shown in Fig. 20. The same behavior is analyzed to NN with enhancing of Reynolds numbers & volume concentrations. NN enhances by increasing different wall temperatures and Reynolds numbers. It can be seen that with a wall temperature of 90°C has a maximum Nusselt no. value than other types & pure water, which agrees with.

Table 12: Nusselt number at different wall temperature for Al_2O_3

Reynolds number	Al_2O_3				
	Pure water	60°C	70°C	80°C	90°C
	Nusselt number				
10000	28.42	48.22	54.34	62.29	75.24
20000	34.63	55.64	69.52	74.45	82.07
40000	45.29	62.82	74.46	80.26	89.34
60000	55.01	72.17	78.29	88.78	98.57
80000	62.58	80.28	85.66	96.46	109.63
100000	69.74	89.36	90.41	102.17	127.52

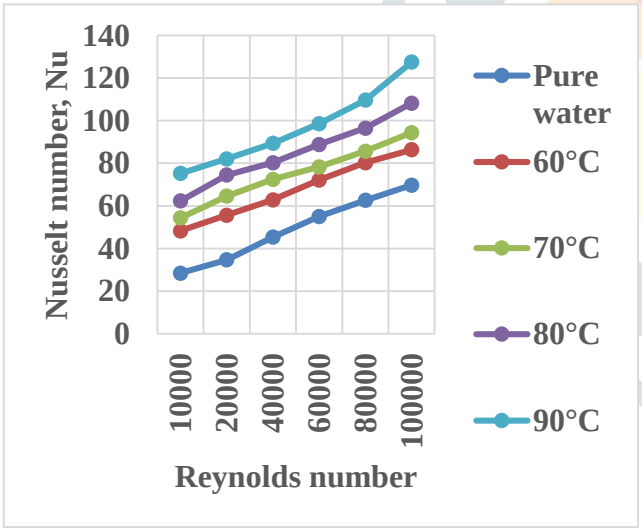

Fig. 21: Variation of Nusselt number at different wall temperature for Al_2O_3

The impact of several wall temperatures on NN is illustrated in Figure 5. The same behavior is observed for Nusselt no. by enhancing volume concentrations and Reynolds numbers. NN enhances by increasing different wall temperatures & Reynolds number. It can be seen that with a wall temperature of 90°C has the most NN value than different types & pure water, which allows with.

FRICTION FACTOR

Table 13: Friction factor at different wall temperature for TiO_2

Reynolds number	TiO_2				
	Pure water	60°C	70°C	80°C	90°C
	Friction factor				
10000	0.215	0.323	0.337	0.348	0.378
20000	0.156	0.257	0.275	0.314	0.348
40000	0.132	0.204	0.232	0.266	0.307
60000	0.123	0.169	0.192	0.242	0.273
80000	0.117	0.143	0.166	0.221	0.252
100000	0.109	0.122	0.152	0.195	0.239

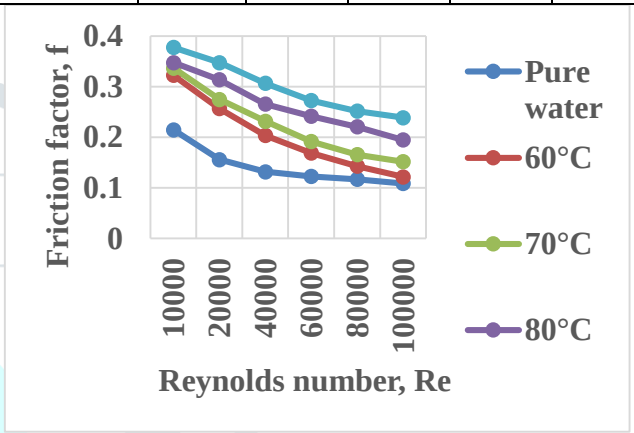

Fig 22: Variation of friction factor at different wall temperature for TiO_2

Figure 22 illustrates the impact of inlet temperature on FF of TiO_2 nanofluid by volume concentrations of 1 percent. It looks that enhancing inlet temp. Causes to decrease in FF.

Table 14: Friction factor at different wall temperature for Ag/HEG

Reynolds number	Ag/HEG				
	Pure water	60°C	70°C	80°C	90°C
	Friction factor				
10000	0.231	0.331	0.342	0.365	0.395
20000	0.167	0.268	0.297	0.321	0.348
40000	0.144	0.216	0.258	0.285	0.315
60000	0.135	0.182	0.225	0.262	0.292
80000	0.124	0.155	0.196	0.243	0.275
100000	0.115	0.138	0.178	0.22	0.258

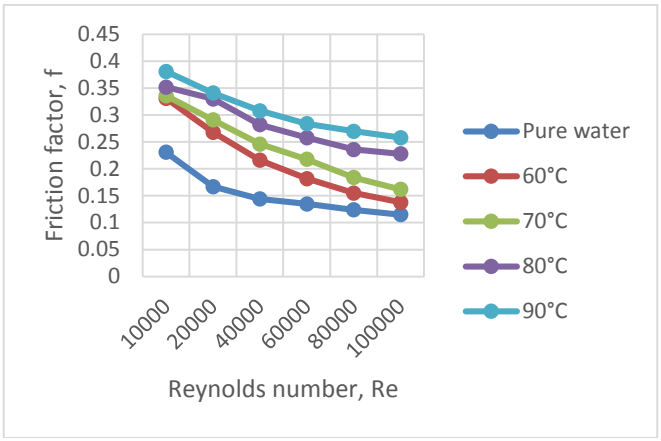

Fig. 23: Friction factor at different wall temperature for Ag/HEG

Figure 23 illustrates the impact of inlet temp. On FF of Ag/HEG nanofluid by volume concentrations of 1%. It looks that enhancing inlet temp. Causes to decrease in FF.

Table 15: Friction factor at different wall temperature for SiO_2

Reynolds number	SiO_2				
	Pure water	60°C	70°C	80°C	90°C
	Friction factor				
10000	0.228	0.328	0.334	0.353	0.376
20000	0.168	0.263	0.283	0.293	0.322
40000	0.142	0.211	0.242	0.265	0.288
60000	0.124	0.175	0.196	0.222	0.267
80000	0.11	0.151	0.184	0.206	0.242
100000	0.105	0.132	0.164	0.179	0.208

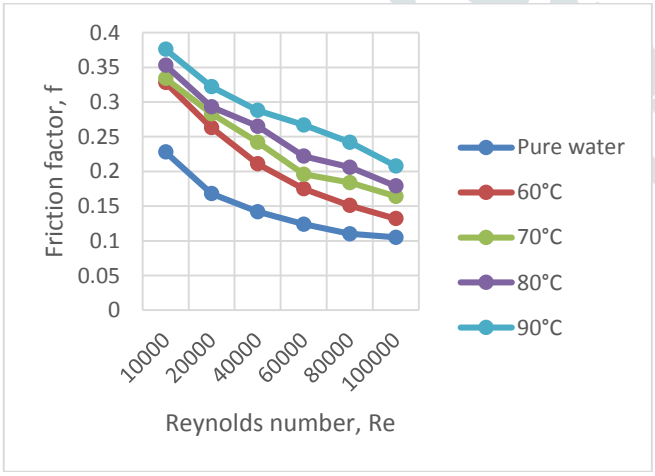

Fig. 24: Variation of friction factor at different wall temperature for SiO_2

Figure 24 shows that the FF effects of SiO2 nanofluid with a volume concentration of 1% are affected by inlet temperature. It appears that an increase in inlet temperature causes FF to decrease.

Table 4.15: Friction factor at different wall temperature for Al_2O_2

Reynolds number	Al_2O_3				
	Pure water	60°C	70°C	80°C	90°C
	Friction factor				
10000	0.231	0.268	0.335	0.354	0.372
20000	0.167	0.213	0.284	0.321	0.336
40000	0.144	0.204	0.246	0.275	0.321
60000	0.135	0.162	0.202	0.242	0.286
80000	0.124	0.148	0.184	0.231	0.279
100000	0.115	0.129	0.167	0.211	0.232

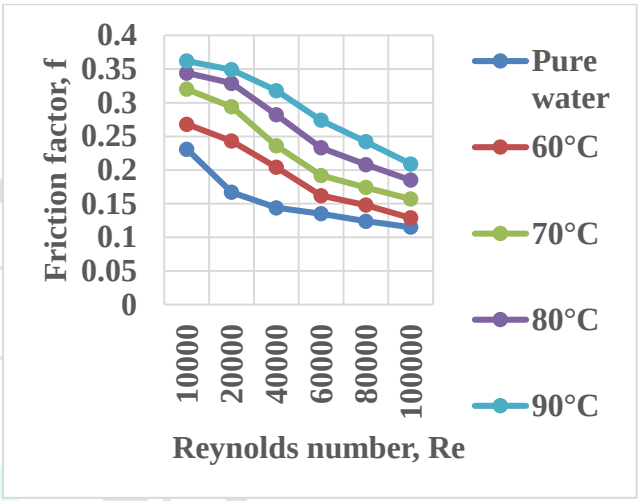

Figure 25: Variation of friction factor at different wall temperature for Al_2O_3

Fig. 25 indicates that the temperature inlet effect on the Al_2O_3 nanofluid friction factor is 1% by volume concentrations. The increase in the entrance temperature tends to cause the friction factor to be that.

V. CONCLUSION

The following conclusion can be drawn from the following studies:

1. FF & HT of forced convection improvement of various nanoparticles suspended in water were defined.
2. When nanoparticles of different concentrations in volume were added to base fluid, significant improvements in FF & HT were perceived.
3. Simulation results (SR) demonstrated that FF & NN behavior of nanofluids were highly based on volume concentration, Reynolds no. & inlet temperature.
4. The results revealed that nanofluid (Ag / HEG) has the highest friction factor of 4 percent in all Reynolds numbers.
5. This approach offers engineers with innovative ways to increase highly dense automotive heat exchangers & heaters. If nanoparticles like water are added to base fluid, the potential increase in cooling rates for car engines could mean that more engine heat could be removed or that cooling systems were reduced by size.
6. Smaller cooling systems will produce smaller & lighter radiators, benefiting almost all aspects of car performance & enhance fuel economy.

REFERENCES

[1] Said, Z., Assad, M. E. H., Hachicha, A. A., Bellos, E., Abdelkareem, M. A., Alazaizeh, D. Z., & Yousef, B. A. (2019). Enhancing the performance of automotive radiators using nanofluids. Renewable and Sustainable Energy Reviews, 112, 183-194.

[2] Gakare, A., Sharma, A., & Saxena, G. (2019). Review of Recent Automotive Experimental Applications of Nano Coolants. Journal of Nanoscience Nanoengineering and Applications, 9(1), 1-10.

[3] Kumar, A., & Subudhi, S. (2019). Preparation, characterization, and heat transfer analysis of nanofluids used for engine cooling. Applied Thermal Engineering, 114092.

[4] Hussein, A. M., Dawood, H. K., Bakara, R. A., & Kadirgamaa, K. (2017). Numerical study on turbulent forced convective heat transfer using nanofluids TiO 2 in an automotive cooling system. Case Studies in Thermal Engineering, 9, 72–78. DOI:10.1016/j.csite.2016.11.005

[5] S. Kumar, S. Chakrabarti, "A Review: Enhancement of Heat Transfer with Nanofluids" International Journal of Engineering Research & TechnologyVol. 3 Issue 4, April - 2014

[6] M. Kh. Abdolbaqi, C.S.N. Azwadi, R. Mamat, W.H. Azmi and G. Najafi, "NANOFLUIDS HEAT TRANSFER ENHANCEMENT THROUGH STRAIGHT CHANNEL UNDER TURBULENT FLOW", ISSN: 2229-8649 (Print); ISSN: 2180-1606 (Online); Volume 11, pp. 2294-2305, January-June 2015

[7] C. K. Sinz, H. E. Woei, M. N. Khalis and S. I. Ali Abbas, "Numerical Study on Turbulent Force Convective Heat Transfer of Hybrid Nanofluid, Ag/HEG in a Circular Channel with Constant Heat Flux", Journal of Advanced Research in Fluid Mechanics and Thermal Sciences ISSN (online): 2289-7879 | Vol. 24, No. 1. Pages 1-11, 2016

[8] Palaniappan, B., & Ramasamy, V. (2019). Thermodynamic analysis of fly ash nanofluid for automobile (heavy vehicle) radiators. Journal of Thermal Analysis and Calorimetry, 136(1), 223-233.

[9] Xian, H. W., Sidik, N. A. C., & Najafi, G. (2019). Recent state of nanofluid in automobile cooling systems. Journal of Thermal Analysis and Calorimetry, 135(2), 981-1008.

[10] Saxena, G., & Soni, P. (2018). Nano Coolants for Automotive Applications: A Review. Nano Trends-A Journal of Nano Technology & Its Applications, 20(1), 9-22.

[11] Micali, F., Milanese, M., Colangelo, G., & de Risi, A. (2018). Experimental investigation on 4-strokes biodiesel engine cooling system based on nanofluid. Renewable energy, 125, 319-326.

[12] Boopathi, P., Venkatachalam, R., Nedunchezhian, N., Subramanian, R., Manikalithas, P., & Bharathiraja, M. (2018). A Novel Fly ash Nanofluid for Automobile Engine Cooling Applications-Preparation and Comparative Studies on Properties.

[13] Shete, D. S., Powar, R. S., & Desai, N. S. Potential of Use of Nanoparticle in Automotive System-A Review.

[14] Wong, K. V., & De Leon, O. (2017). Applications of nanofluids: current and future. In Nanotechnology and Energy (pp. 105-132). Jenny Stanford Publishing.

[15] Sidik, N. A. C., Yazid, M. N. A. W. M., & Mamat, R. (2017). Recent advancement of nanofluids in the engine cooling system. Renewable and Sustainable Energy Reviews, 75, 137-144.

[16] Molana, M. (2017). On the nanofluids application in the automotive radiator to reach the enhanced thermal performance: a review. American Journal of Heat and Mass Transfer, 4(4), 168-187.

[17] Sahoo, R. R., & Sarkar, J. (2017). Heat transfer performance characteristics of hybrid nanofluids as coolant in louvered fin automotive radiator. Heat and Mass Transfer, 53(6), 1923-1931.

[18] Devireddy, S., Mekala, C. S. R., & Veeredhi, V. R. (2016). Improving the cooling performance of automobile radiator with ethylene glycol water-based TiO2 nanofluids. International communications in heat and mass transfer, 78, 121-126.

[19] Baskar, S., & Rajaraman, R. (2015). Airflow Management in Automotive Engine Cooling System Overview. International Journal of Thermal Technologies, 5(1), 1-8.